Recognition-Control and Host-Guest Interactions in High-Symmetry Cocrystals of Fullerenes with Cubane and Mesitylene

Gábor Bortel[*1], *Éva Kováts*[1], *Dávid Földes*[1,2], *Emma Jakab*[3], *Gábor Durkó*[4] *and Sándor Pekker*[1,5]

[1]Institute for Solid State Physics and Optics, Wigner Research Centre for Physics, P.O.Box 49, H-1525 Budapest, Hungary

[2]Doctoral School on Materials Sciences and Technologies, Óbuda University, Bécsi út 96/b, H-1034 Budapest, Hungary

[3]Institute of Materials and Environmental Chemistry, Research Centre for Natural Sciences, P.O.Box 17, H-1525 Budapest, Hungary

[4]Department of Organic Chemistry, Eötvös Loránd University, P.O.Box 32, H-1518 Budapest, Hungary

[5]Faculty of Light Industry and Environmental Engineering, Óbuda University, Doberdó út 6, H-1034 Budapest, Hungary

* E-mail: bortel.gabor@wigner.mta.hu

The limited success in the prediction of structure is one of the most serious problems in the engineering of molecular crystals. Here we show that the packing of high-symmetry molecules such as ball-shaped rotating fullerenes, cube-shaped cubane and octahedral-shaped mesitylene dimers give rise to the formation of cubic cocrystals with easily predictable lattice parameters. We present the synthesis and structure determination of $Sc_3N@C_{80}$-I_h cocrystals with cubane (C_8H_8) and mesitylene (C_9H_{12}) and compare the new materials with related C_{60} and C_{70} based structures. In this family of materials, most atom-to-atom interactions are averaged out by the symmetry and the crystal structures can be described in terms of classical molecule-to-molecule interactions. Size-dependent homo- and heteromolecular contacts control the stability of the ball-cube and ball-octahedron systems creating several host-guest and recognition-controlled regions. The analysis of the global phase diagrams explains not only the stability of the observed materials, but also the instability of a missing derivative.

Table of Contents / Abstract graphic

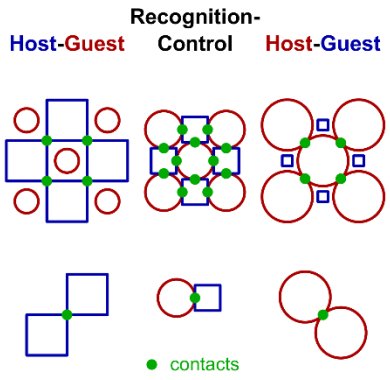

Supramolecular Interactions, Crystal Engineering, Cocrystal Structure, Cohesion Energy, Fullerenes, Cubane, Mesitylene

Multicomponent crystals of organic and inorganic molecules represent one of the mostly studied families of cocrystals for their great pharmaceutical importance [1, 2, 3, 4]. The intensive studies of the structure and the thermodynamics of formation [5, 6, 7] contributed to the better understanding of these systems, but the rational design of new cocrystals has remained an unresolved challenge [8, 9]. The structure of molecular crystals is usually controlled by local atom-atom contacts of the nearest neighbor molecules with often irregular surfaces [10], resulting in the formation of low-symmetry structures [11]. The flexibility of constituents and the great variety of these interactions make it very difficult, practically still impossible, to predict crystal structures [12]. On the other hand, high-symmetry, rigid molecules, or disordered systems with increased effective molecular symmetry (e.g., a rotating molecule or group) give rise to high-symmetry structures. In case of cocrystals, homo- and heteromolecular atom-atom interactions can have equal importance in the stabilization of these structures, distinguishing cocrystals from host-guest systems, stabilized predominantly by homomolecular interactions. Constituents of identical effective molecular shapes may also exist in different sizes that typically lead to isostructurality [13]. The cocrystals of large ball-shaped molecules, like fullerenes [14] or carboranes [15, 16] represent a special group with interactions controlled by the recognition of complementary surfaces [17, 18, 19]. The study of supramolecular interactions in series of such isostructural high-symmetry cocrystals facilitated by the limited number of free variables may contribute to better understanding of the structures, classifies them into host-guest or recognition-controlled categories, allows the separation of the shape and size effects, makes possible the design of related materials and predicts their physical properties.

Freely rotating fullerenes [14], C_{60}, C_{70} and $Sc_3N@C_{80}$ (**1**) (trimetallic nitride endohedral fullerene, the next fullerene of icosahedral symmetry after C_{60}) [20, 21, 22, 23] have average

spherical shape of nanometer size, resulting in face-centered cubic (FCC) molecular crystal structures at ambient or slightly elevated temperatures [24]. The close-packed arrays with large sizes of voids are able to accommodate small molecules; therefore, fullerenes readily form cocrystals with a great variety of organic and inorganic molecules [16]. However, only a few guest molecules of appropriate shape and size can maintain and stabilize high-symmetry structures.

Fullerene-cubane cocrystals represent one of the highest possible symmetry heteromolecular systems [25, 26, 27]. The effective shape and size recognition of the complementary molecular surfaces of the slightly concave cubanes [28, 29, 30] and the spherical fullerenes gives rise to unusual crystal dynamics, the so-called rotor-stator properties [25, 31]. The structure and the dynamics of this family of materials depend on the size and the symmetry of the fullerene component. As the icosahedral $Sc_3N@C_{80}$ stands closest to an effective spherical shape among larger fullerenes, the next expected member of the fullerene-cubane series is the $Sc_3N@C_{80}$•C_8H_8 (**2**). This cocrystal was prepared and characterized for the first time.

A complementary family of the fullerene-cubane phases is the fullerene-mesitylene system, consisting of matching spherical and octahedral units. The supramolecular dimer of mesitylene has a slightly distorted octahedral shape that can stabilize a primitive cubic (PC) arrangement of various fullerenes. The prototype of this new family of high-symmetry fullerene cocrystals is C_{70}•$(C_9H_{12})_2$ (**3**) [32]. The existence of isostructural cocrystals with smaller or larger fullerenes or the nature of their supramolecular interactions have not been studied yet.

Here we analyze the scaling of major structural characteristics with molecule size in two complementary families of the highest possible symmetry fullerene cocrystals, the NaCl (B1) type fullerene-cubane and the CsCl (B2) type fullerene-mesitylene systems. First, we report on

the formation, structure and stability of two missing members of these families, the cocrystals of $Sc_3N@C_{80}$ (**1**) with cubane: $Sc_3N@C_{80}•C_8H_8$ (**2**) and with mesitylene: $Sc_3N@C_{80}•(C_9H_{12})_2$ (**4**). Then we compare the new structures with the previously reported C_{60} and C_{70} cocrystals, as well as with the FCC crystals of the parent fullerenes. We discuss the size-dependence of the homo- and heteromolecular interactions in both families and define the structural conditions for formation of recognition-controlled cocrystals or host-guest systems. We show that all 3 fullerene-cubane cocrystals belong to the former, while the high-symmetry fullerene-mesitylene crystals to the latter group. Based on our analysis, we also explain the easy formation and high stability of $C_{70}•(C_9H_{12})_2$ (**3**), the lower than expected lattice parameter of $Sc_3N@C_{80}•(C_9H_{12})_2$ (**4**) and the formation of a differently packed, lower-symmetry structure of $(C_{60})_2•C_9H_{12}$ (**5**) instead of an isostructural C_{60} cocrystal. Beside the preparation, thermogravimetry – mass spectrometry (TG-MS) and x-ray powder diffraction (XRPD) experiments, we provide geometrical model and cohesion energy calculations to support our experimental findings. We end up with a short outlook of our analysis of supramolecular interactions in terms of other approaches, like Hirshfeld surface analysis [33, 34]. The results of experimental methods and model calculations are summarized in Table 1; for the details see the Supporting Information (SI).

The microcrystalline powder of $Sc_3N@C_{80}•C_8H_8$ (**2**) precipitated from toluene solution of the components is stable up to 200 ºC (Figure S1). It has a rocksalt structure of orientationally disordered fullerenes and orientationally ordered cubanes (Figures 1a and S5), similarly to the structures of previous high-symmetry members of the fullerene-cubane cocrystals [25]. The present results are consistent with either freely rotating fullerenes or an orientational glass of static fullerenes.

$Sc_3N@C_{80}•(C_9H_{12})_2$ (**4**), a new member of the fullerene-mesitylene family, was prepared via the crystallization of $Sc_3N@C_{80}$ (**1**) from its mesitylene solution, similarly to C_{70}-mesitylene cocrystal, reported previously [32]. TG-MS results indicate the stability with 1:2 composition up to 100 ºC, where decomposition starts to take place in 2 steps via a metastable phase with 2:1 composition at 180 ºC (Figure S3). According to the XRPD data (Figure S6), $Sc_3N@C_{80}•(C_9H_{12})_2$ (**4**) is isostructural to the C_{70}-mesitylene [32]: fullerenes form a PC sublattice, with a mesitylene dimer in the center of the unit cell (Figure 1b). Based on the considerations given below this structure consists of merohedrally disordered fullerenes and has $Pm\bar{3}m$ space group. Free rotation, or complete static orientational disorder of fullerenes is excluded.

In order to investigate its stability, $C_{70}•(C_9H_{12})_2$ (**3**), the already known member of the fullerene-mesitylene family was also prepared and its structure confirmed by XRPD. The 2-step decomposition path on the TG-MS curve (Figure S2) similar to that of $Sc_3N@C_{80}•(C_9H_{12})_2$ (**4**) indicates that both $(C_{70})_2•C_9H_{12}$ and $(Sc_3N@C_{80})_2•C_9H_{12}$ may also exist, at least in metastable forms. A crystallization attempt of the missing C_{60}-mesitylene cocrystal resulted in the formation of lower symmetry cocrystals of $(C_{60})_2•C_9H_{12}$ (**5**). Rietveld fit of the XRPD data (Figure S7) indicates a hexagonal structure closely related to that of the C_{60}-m-xylene and C_{60}-toluene [35, 36, 37], that is completely different from the cubic C_{70} and C_{80} derivatives (Figure S8). Upon heating, this material decomposed to C_{60} in a single step between 150-230 ºC (Figure S4).

Two main structural properties of the above materials, the lattice parameter and the space filling (volume fraction occupied by molecules) as a function of the effective fullerene diameter display the nature of the supramolecular interactions in a spectacular way (Figures 2 and 3). In a geometrical model, where spheres, cubes and truncated octahedrons represent fullerenes,

cubanes and mesitylene dimers, respectively, the cubic lattice parameter is given as the maximum of 3 terms representing various touching conditions (see the SI, the TOC figure and the solid lines in Figures 2 and 3). If the maximum is controlled by one of the homomolecular contacts, the contacting molecules form a host lattice for the other constituent located as guest among them. On the other hand, if it is controlled by the heteromolecular contact, both constituents are crucial and the structure, dynamics and stability is controlled by their shape and size recognition.

Quantitative explanation of the experimental data requires to exceed the geometrical approach and to consider molecular interactions. While the geometric model returns continuous functions for structural parameters, a cohesion energy calculation provides discrete values for given molecules via optimization. The precise calculated lattice parameters are obtained at the minimum of the total cohesion energies calculated from summation of van der Waals and Coulomb potentials as described in previous publications [38, 27, 24] and in the SI. The measured and optimized structural parameters of the crystals are summarized in Table 1, and are shown together with the graphical representation of the geometrical model, as a function of the effective van der Waals diameter of the fullerenes (Figures 2 and 3). In terms of this electrostatic potential calculations, the recognition-control regime is where the heteromolecular terms dominate the repulsion, and the host-guest region is where the homomolecular interaction of one of the constituents dominates.

The recognition-controlled nature of all members of the FCC fullerene-cubane system is indicated by the results shown in Figure 2a. The lines represent the 3 terms of the geometrical model; the solid line is the actual maximum. A slight deviation of this model from the data points is due to neglecting the concave cubane faces. The lattice parameters of the parent fullerenes

calculated by the pair potential method are identical to those of the optimized values of the fullerene sublattices in the fullerene-cubane cocrystals, which are also plotted in Figure 2a. The lattice parameters of all 3 fullerene-cubane cocrystals are higher, both sublattices are expanded in the cocrystals. This implies that the fullerene-cubane heteromolecular contacts are under compression; they keep balance with the expanded fullerene-fullerene and the cubane-cubane homomolecular contacts. The cubic symmetry of the fullerene-cubane cocrystals is stabilized by the almost perfect match of the complementary molecular surfaces in a wide range of fullerene diameters, hence is the name recognition-controlled regime. This shape recognition can only be realized between the surfaces of rotating fullerenes and static cubanes, as the rectangular atomic arrangement of the cubane faces cannot match the hexagonal-pentagonal pattern of the fullerene surfaces. If this condition is not met, the symmetry is lowered, as it was observed in the case of low temperature structures of C_{60}- and C_{70}-cubane cocrystals [26, 27]. This effect of molecular bearing also gives rise to enhanced rotation of fullerenes with unusually low orientational ordering temperature [25]. Although all three cubane cocrystals are in the recognition-controlled regime, the two approaching lines cross each other at $d = 11.55$ Å, where a host sublattice of the touching fullerene balls forms, and the cocrystal becomes a host-guest structure. Previously, this critical value was estimated for C_{88} [39]. The present experimental and calculated lattice parameters of $Sc_3N@C_{80}$•C_8H_8 (**2**) confirm this model. The isostructural cubane cocrystals of larger fullerene diameter are predicted to be host-guest structures with the same or – due to fullerene-cubane attraction – even smaller lattice parameter, as their parent fullerene structure.

The change in the nature of the structure at the critical diameter is more striking, if we plot the space filling as a function of the effective fullerene diameter (Figure 2b). For the parent FCC structures it is constant 0.74 ($\pi/3\sqrt{2}$), while for the 3 cocrystals shows increasing values. At the

critical fullerene diameter, where the match of the fullerenes and cubanes is optimal, it takes a maximal value of 0.84. Beyond that point it starts to decrease due to cubane molecules that do not completely fill the octahedral voids.

Another good cocrystal series to study the size dependence of supramolecular interactions is the fullerene-mesitylene system that is somewhat more complicated. The primary difference is that both the fullerene and the mesitylene form unstable PC sublattices; their parent structure does not exist. The cocrystal structure can only be stabilized by heteromolecular interactions; high-symmetry structures can only form at a narrow range of molecular sizes. Furthermore, the supramolecular mesitylene dimer is not a rigid molecule; thus, the distance of the monomers is able to compensate for changes in the interactions with the adjacent fullerenes. The PC lattice parameter as a function of effective fullerene diameter is shown in Figure 3a. Here – in contrast to the case of cubane – the recognition-controlled regime is rather narrow and all 3 lines representing the geometrical model are visible. Far away from this region new solutions are found to yield stable host-guest systems, as it will be shown below.

In the hypothetic C_{60}•$(C_9H_{12})_2$ PC structure the mesitylene sublattice is compressed and the fullerene sublattice is expanded by about 0.25 Å. If this structure existed, it would be a mesitylene host framework containing fullerene guest molecules. However, mesitylene dimers cannot survive any compression at the vertices of the octahedrons. This flexibility may be the primary reason that this structure does not exist, but a significantly different, hexagonal structure with lower symmetry, less effective packing and different composition is realized in $(C_{60})_2$•C_9H_{12} (**5**) (Figure S7 and S8).

The crossing points of the lattice parameters in Figure 3a at $d = 10.40$ Å and $d = 10.58$ Å enclose a narrow recognition-controlled region, where heteromolecular interactions dominate.

Although there is no high-symmetry fullerene here, C_{70}•$(C_9H_{12})_2$ (**3**) is very close to the upper crossing point.

Above this region, the mesitylene sublattice is expanded; the adjacent dimers attract each other. Fullerenes form host systems of slightly repulsive nearest neighbor molecules for the mesitylene dimer guests. In the case of C_{70} cocrystal, the difference between the lattice parameters of the sublattices and that obtained from the optimized fullerene-mesitylene interaction is as low as 0.02 Å, showing that both supramolecular interactions have equal importance in the stabilization of the structure. Thus, cocrystal C_{70}•$(C_9H_{12})_2$ (**3**) is considered an ideal host-guest system where the mesitylene guest molecules occupy the full volume of the voids of the host framework. The small mismatch can be the reason of the observed lowering of the symmetry from $Pm\bar{3}m$ to $P\bar{4}3m$ [32]. $Sc_3N@C_{80}$•$(C_9H_{12})_2$ (**4**) is a similar host-guest system; however, the experimental lattice parameter of the cocrystal is 0.13 Å smaller, than the van der Waals diameter, i.e. the nearest neighbor distance of rotating fullerenes. Such a huge compression is inconsistent with rotating or orientationally disordered fullerenes. This controversy is resolved by merohedral disorder [14] of fullerenes (Figure 1b). In the two orientations all nearest neighbor fullerenes are facing each other with hexagons and the smallest spatial extent of the cage along the cubic lattice directions results in a triply flattened effective molecular shape and brings the lattice parameter in agreement with the experimental value. (This is exactly the opposite of the also icosahedral C_{60}, where merohedral disorder makes the 6–6 bonds protuberate at the cubic lattice directions.) A 3D checkered array of fullerenes in alternating standard orientations is excluded by the absence of superreflections from the XRPD data (Figure S6). Both the 4-fold disorder of the mesitylene dimers on the 8 faces of the octahedron and the 2-fold merohedral disorder of fullerenes are consistent with the $Pm\bar{3}m$ space

group symmetry, there is no indication of lowering to $P\bar{4}3m$. Despite its larger average size, $Sc_3N@C_{80}•(C_9H_{12})_2$ (**4**) is also an ideal host-guest system. The hexagon-to-hexagon contacts of the fullerenes stabilize the cubic structure of the host framework, while the mesitylene dimers of slightly increased intermolecular distances fully occupy the voids of the framework. This partially ordered stationary structure forecasts an orientational phase transition above room temperature, if no decomposition takes place before.

The ideal host-guest character of $C_{70}•(C_9H_{12})_2$ (**3**) and $Sc_3N@C_{80}•(C_9H_{12})_2$ (**4**) cocrystals is also indicated by their space filling ratios (Figure 3b). Both values are around the maximal 0.85 value reached at the crossover with the recognition-controlled regime. For comparison, this is far the largest of 0.52 ($\pi/6$) for the PC fullerene sublattice, 0.74 for the FCC fullerene sublattice and 0.80 for the FCC fullerene-cubane structures, indicating that these are the most compact structures.

Large deviation of the experimental and the optimized lattice parameter and space filling ratios from the values predicted by the geometrical model is a sign of a strongly strained structure that requires high cohesion energy. In the case of mesitylene cocrytals this properly indicated the non-existence of PC cocrystals of $C_{60}•(C_9H_{12})_2$ and excluded the complete orientational disorder in $Sc_3N@C_{80}•(C_9H_{12})_2$ (**4**).

It is instructive to compare our results with the Hirshfeld surface analysis [33, 34] widely applied in the field of crystal engineering. In the latter method, some quantity, typically the d_{norm} values characterizing local interactions are plotted on a molecular surface representing the boundary of a molecule in a structure (Figure 4). Negative and positive values – commonly shown in red and blue colors [40] – indicate repulsion and attraction, respectively. This representation spectacularly shows the local contribution of the atom pairs to the total interaction

of the molecule with its neighbors; however, it does not provide quantitative information on the overall supramolecular interaction. We can equally see repulsion and attraction in the fullerene–fullerene, the fullerene–cubane/mesitylene and in the mesitylene–mesitylene interaction regions of the Hirshfeld surfaces of $Sc_3N@C_{80}•C_8H_8$ (**2**) (Figure 4a) and $Sc_3N@C_{80}•(C_9H_{12})_2$ (**4**) (Figure 4b). However, we cannot estimate the direction or the magnitude of the overall intermolecular interactions (repulsion vs. attraction) and how they balance each-other in the complete structure. We cannot derive the value of the lattice parameter and decide which molecule pairs dominate in defining the size of the lattice. On the other hand, in the course of our calculations we evaluate the fractional contributions to the total interaction energy (at molecular level) and this makes possible to separate sublattice interactions. This sheds light on how the supramolecular pair interactions ultimately control the stability and lattice parameter of the complete structure and clearly identifies the cocrystal as being in the host-guest or the recognition-controlled regime.

In conclusion, we have systematically analyzed the supramolecular interactions in several high-symmetry members of two fullerene cocrystal families and provided a consistent model that explains the size dependence of the structural parameters and stability. To complete the family, we prepared and characterized new high symmetry cocrystals of an endohedral trimetallic nitride derivative of C_{80}, the B1 type $Sc_3N@C_{80}•C_8H_8$ (**2**), and the B2 type $Sc_3N@C_{80}•(C_9H_{12})_2$ (**4**). The cubic structure of the cubane cocrystal is stabilized by the effective shape recognition at all 3 fullerene sizes. In the mesitylene cocrystals unstable PC frameworks are stabilized by the dimers of mesitylene. The smaller-than-expected unit cell of the largest fullerene cocrystal is explained with the hexagon-hexagon contacts of merhohedrally disordered fullerenes. The calculated supramolecular interactions exclude the possibility of a corresponding cubic cocrystal of C_{60}, that is confirmed by the successful preparation of hexagonal cocrystals with entirely different

packing and composition of $(C_{60})_2 \bullet C_9H_{12}$ (**5**). The approach of sublattice optimization can be applied to any cocrystals of rigid constituents, even at lower hexagonal, tetragonal or orthorhombic symmetry, to reveal how the fractional contributions of supramolecular interactions contribute to the stability of a cocrystal. This know-how is also beneficial at assessing the existence of hypothetic cocrystals in crystal structure engineering for specific applications.

Acknowledgement. É.K. gratefully acknowledges the support from the National Research, Development and Innovation Office - NKFIH FK-125063.

Supporting Information. Details and results of all experimental and calculation methods (suppinf.pdf), Crystallographic information files of the new structures, also deposited at The Cambridge Crystallographic Data Centre (Sc3NC80_cubane.cif CCDC#1984479, Sc3NC80_mesitylene.cif CCDC#1984486, C60_mesitylene.cif CCDC#1984478).

References

[1] G. Desiraju, *Crystal Engineering: The Design of Organic Solids (Materials Science Monographs)*. Elsevier Science, 1989.

[2] G. P. Stahly, "A survey of cocrystals reported prior to 2000" *Crystal Growth & Design*, vol. 9, pp. 4212–4229, oct 2009.

[3] S. Aitipamula, R. Banerjee, A. K. Bansal, K. Biradha, M. L. Cheney, A. R. Choudhury, G. R. Desiraju, A. G. Dikundwar, R. Dubey, N. Duggirala, P. P. Ghogale, S. Ghosh, P. K. Goswami, N. R. Goud, R. R. K. R. Jetti, P. Karpinski, P. Kaushik, D. Kumar, V. Kumar, B. Moulton, A. Mukherjee, G. Mukherjee, A. S. Myerson, V. Puri, A. Ramanan, T. Rajamannar,

C. M. Reddy, N. Rodriguez-Hornedo, R. D. Rogers, T. N. G. Row, P. Sanphui, N. Shan, G. Shete, A. Singh, C. C. Sun, J. A. Swift, R. Thaimattam, T. S. Thakur, R. K. Thaper, S. P. Thomas, S. Tothadi, V. R. Vangala, N. Variankaval, P. Vishweshwar, D. R. Weyna, and M. J. Zaworotko, "Polymorphs, salts, and cocrystals: What's in a name?" *Crystal Growth & Design*, vol. 12, pp. 2147–2152, apr 2012.

[4] N. K. Duggirala, M. L. Perry, Ö. Almarsson, and M. J. Zaworotko, "Pharmaceutical cocrystals: along the path to improved medicines" *Chemical Communications*, vol. 52, no. 4, pp. 640–655, 2016.

[5] S. S. L. Price, "Quantifying intermolecular interactions and their use in computational crystal structure prediction" *CrystEngComm*, vol. 6, no. 61, p. 344, 2004.

[6] J. H. ter Horst, M. A. Deij, and P. W. Cains, "Discovering new co-crystals" *Crystal Growth & Design*, vol. 9, pp. 1531–1537, mar 2009.

[7] A. Kitaigorodsky, *Molecular crystals and Molecules*. Academic Press, 2012.

[8] J. Maddox, "Crystals from first principles" *Nature*, vol. 335, pp. 201–201, sep 1988.

[9] G. R. Desiraju, "Cryptic crystallography" *Nature Materials*, vol. 1, pp. 77–79, oct 2002.

[10] M. A. Spackman and P. G. Byrom, "A novel definition of a molecule in a crystal" *Chemical Physics Letters*, vol. 267, pp. 215–220, mar 1997.

[11] E. Prince, ed., *International Tables for Crystallography,Volume C: Mathematical, Physical and Chemical Tables,* Chapter 9.7. Springer, 2004.

[12] G. M. Day and C. H. Görbitz, "Introduction to the special issue on crystal structure prediction" *Acta Crystallographica Section B Structural Science, Crystal Engineering and Materials*, vol. 72, pp. 435–436, aug 2016.

[13] A. Authier, ed., *International Tables for Crystallography,Volume D: Physical properties of crystals,* Chapter 3.3. Springer, 2003.

[14] M. S. Dresselhaus, G. Dresselhaus, and P. C. Eklund, *Science of Fullerenes and Carbon Nanotubes: Their Properties and Applications*. Academic Press, 1996.

[15] M. J. Hardie and C. L. Raston, "Confinement and recognition of icosahedral main group cage molecules: fullerene C_{60} and o-, m-, p-dicarbadodecaborane(12)" *Chemical Communications*, no. 13, pp. 1153–1163, 1999.

[16] I. S. Neretin and Y. L. Slovokhotov, "Chemical crystallography of fullerenes" *Russian Chemical Reviews*, vol. 73, pp. 455–486, may 2004.

[17] S. Stevenson, G. Rice, T. Glass, K. Harich, F. Cromer, M. R. Jordan, J. Craft, E. Hadju, R. Bible, M. M. Olmstead, K. Maitra, A. J. Fisher, A. L. Balch, and H. C. Dorn, "Small-bandgap endohedral metallofullerenes in high yield and purity" *Nature*, vol. 401, pp. 55–57, sep 1999.

[18] S. Stevenson, J. P. Phillips, J. E. Reid, M. M. Olmstead, S. P. Rath, and A. L. Balch, "Pyramidalization of Gd_3N inside a C_{80} cage. the synthesis and structure of $Gd_3N@C_{80}$" *Chemical Communications*, no. 24, p. 2814, 2004.

[19] A. Sygula, F. R. Fronczek, R. Sygula, P. W. Rabideau, and M. M. Olmstead, "A double concave hydrocarbon buckycatcher" *Journal of the American Chemical Society*, vol. 129, pp. 3842–3843, apr 2007.

[20] T.-S. Wang, L. Feng, J.-Y. Wu, W. Xu, J.-F. Xiang, K. Tan, Y.-H. Ma, J.-P. Zheng, L. Jiang, X. Lu, C.-Y. Shu, and C.-R. Wang, "Planar quinary cluster inside a fullerene cage: Synthesis and structural characterizations of $Sc_3N@C_{80}$-I_h" *Journal of the American Chemical Society*, vol. 132, pp. 16362–16364, nov 2010.

[21] X. Lu, L. Feng, T. Akasaka, and S. Nagase, "Current status and future developments of endohedral metallofullerenes" *Chemical Society Reviews*, vol. 41, no. 23, p. 7723, 2012.

[22] A. A. Popov, S. Yang, and L. Dunsch, "Endohedral fullerenes" *Chemical Reviews*, vol. 113, pp. 5989–6113, may 2013.

[23] X. Lu, L. Echegoyen, A. L. Balch, S. Nagase, and T. Akasaka, eds., *Endohedral Metallofullerenes: Basics and Applications*. CRC Press, 2014.

[24] G. Bortel, É. Kováts, E. Jakab, and S. Pekker, "Solvent-free $Sc_3N@C_{80}$-I_h and its precursor cocrystal with toluene" *Fullerenes, Nanotubes and Carbon Nanostructures*, vol. 23, pp. 557–565, sep 2014.

[25] S. Pekker, É. Kováts, G. Oszlányi, G. Bényei, G. Klupp, G. Bortel, I. Jalsovszky, E. Jakab, F. Borondics, K. Kamarás, M. Bokor, G. Kriza, K. Tompa, and G. Faigel, "Rotor-stator molecular crystals of fullerenes with cubane" *Nature Materials*, vol. 4, pp. 764–767, sep 2005.

[26] G. Bortel, G. Faigel, É. Kováts, G. Oszlányi, and S. Pekker, "Structural study of C_{60} and C_{70} cubane" *Physica Status Solidi B*, vol. 243, pp. 2999–3003, nov 2006.

[27] G. Bortel, S. Pekker, and E. Kovats, "Low temperature structure and supramolecular interactions of the C_{60}-cubane cocrystal" *Crystal Growth & Design*, vol. 11, pp. 865–874, mar 2011.

[28] P. E. Eaton and T. W. Cole, “The cubane system” *Journal of the American Chemical Society*, vol. 86, pp. 962–964, mar 1964.

[29] P. E. Eaton, N. Nordari, J. Tsanaktsidis, and S. P. Upadhyaya, “Barton decarboxylation of cubane-1,4-dicarboxylic acid: Optimized procedures for cubanecarboxylic acid and cubane” *Synthesis*, vol. 1995, pp. 501–502, may 1995.

[30] T. Yildirim, P. M. Gehring, D. A. Neumann, P. E. Eaton, and T. Emrick, “Unusual structure, phase transition, and dynamics of solid cubane” *Physical Review Letters*, vol. 78, pp. 4938–4941, jun 1997.

[31] C. Bousige, S. Rols, J. Cambedouzou, B. Verberck, S. Pekker, É. Kováts, G. Durkó, I. Jalsovsky, É. Pellegrini, and P. Launois, “Lattice dynamics of a rotor-stator molecular crystal: Fullerene-cubane $C_{60}{\cdot}C_8H_8$” *Physical Review B*, vol. 82, nov 2010.

[32] C. Park, E. Yoon, M. Kawano, T. Joo, and H. C. Choi, “Self-crystallization of C_{70} cubes and remarkable enhancement of photoluminescence” *Angewandte Chemie International Edition*, vol. 49, pp. 9670–9675, nov 2010.

[33] J. J. McKinnon, D. Jayatilaka, and M. A. Spackman, “Towards quantitative analysis of intermolecular interactions with Hirshfeld surfaces” *Chemical Communications*, no. 37, p. 3814, 2007.

[34] M. A. Spackman and D. Jayatilaka, “Hirshfeld surface analysis” *CrystEngComm*, vol. 11, no. 1, pp. 19–32, 2009.

[35] M. Ramm, P. Luger, D. Zobel, W. Duczek, and J. C. A. Boeyens, "Static disorder in hexagonal crystal structures of C_{60} at 100K and 20K" *Crystal Research and Technology*, vol. 31, no. 1, pp. 43–53, 1996.

[36] J. Minato and K. Miyazawa, "Solvated structure of C_{60} nanowhiskers" *Carbon*, vol. 43, pp. 2837–2841, nov 2005.

[37] M. Rana, R. Bharathanatha, and U. K. Gautam, "Kinetically stabilized C_{60}-toluene solvate nanostructures with a discrete absorption edge enabling supramolecular topotactic molecular exchange" *Carbon*, vol. 74, pp. 44–53, aug 2014.

[38] L. A. Girifalco, "Interaction potential for C_{60} molecules" *The Journal of Physical Chemistry*, vol. 95, pp. 5370–5371, jul 1991.

[39] S. Pekker, É. Kováts, G. Oszlányi, G. Bényei, G. Klupp, G. Bortel, I. Jalsovszky, E. Jakab, F. Borondics, K. Kamarás, and G. Faigel, "Rotorstator phases of fullerenes with cubane derivatives: A novel family of heteromolecular crystals" *physica status solidi (b)*, vol. 243, pp. 3032–3036, nov 2006.

[40] M. J. Turner, J. J. McKinnon, S. K. Wolff, D. J. Grimwood, P. R. Spackman, D. Jayatilaka, and M. A. Spackman, "Crystalexplorer17." http://hirshfeldsurface.net, 2017.

Table 1. Space group, experimental and calculated lattice parameters of all discussed fullerene-based crystals. The 5 materials indicated with bold numbers have been prepared and experimentally characterized in this work, (**2**), (**4**) and (**5**) is reported for the first time. Cohesion energy calculations and structure optimizations have been performed for all materials. For mesitylene systems 2 calculated lattice parameters are shown for rotating and merohedrally disordered fullerenes. Underlines indicate the real orientational state. Starting temperatures of thermal decomposition are also listed.

Composition	**C_{60}**	**C_{70}**	**$Sc_3N@C_{80}$**
Pristine Fullerene	$Fm\bar{3}m$ a_{exp} = 14.15 Å a_{calc} = 14.1414 Å	$Fm\bar{3}m$ a_{exp} = 15.01 Å a_{calc} = 15.0184 Å	$Fm\bar{3}m$ (**1**) a_{exp} = 15.61 Å a_{calc} = 15.6498 Å
Fullerene : Cubane 1:1	$Fm\bar{3}m$ a_{exp} = 14.74 Å a_{calc} = 14.7539 Å	$Fm\bar{3}m$ a_{exp} = 15.38 Å a_{calc} = 15.4010 Å	$Fm\bar{3}m$ (**2**) a_{exp} = 15.87 Å a_{calc} = 15.8905 Å stable up to 200 °C
Fullerene : Mesitylene 1:2	$Pm\bar{3}m$ a_{exp} : - (hypothetic) $a_{calc,rot}$ = 10.1540 Å $a_{calc,mero}$ = 10.1381 Å	$P\bar{4}3m$ (**3**) a_{exp} = 10.59 Å $\underline{a_{calc,rot} = 10.5820\ Å}$ $a_{calc,mero}$ = 10.6199 Å stable up to 140 °C	$Pm\bar{3}m$ (**4**) a_{exp} = 10.90 Å $a_{calc,rot}$ = 10.9635 Å $\underline{a_{calc,mero} = 10.8960\ Å}$ stable up to 100 °C
Fullerene : Mesitylene 2:1	$P6_3/m$ (**5**) a_{exp} = 23.77 Å, c_{exp} = 10.19 Å stable up to 150 °C	not isolated, but exists at 200°C as intemediate decomposition product of (**3**)	not isolated, but exists at 180°C as intemediate decomposition product of (**4**)

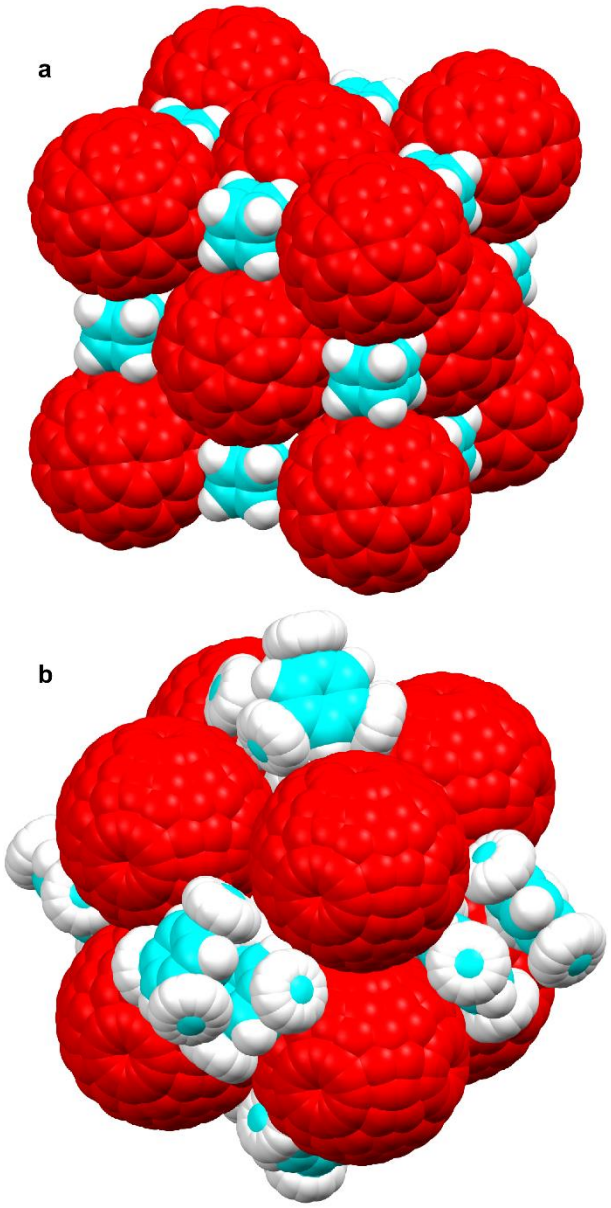

Figure 1. Space fill view of the (a) FCC $Sc_3N@C_{80}•C_8H_8$ (**2**) and the (b) PC $Sc_3N@C_{80}•(C_9H_{12})_2$ (**4**) cocrystals. (a) The orientationally disordered fullerenes are shown in random orientations. The average spherical electron density complies with the highest cubic symmetry. (b) Two standard orientations of the fullerene units are superimposed, representing the merohedral disorder. Mesitylene dimers form octahedra with the common C_3 axes oriented randomly along

the four (111) directions of the lattice, creating an average octahedral electron density. Thus, both constituents comply with the cubic symmetry.

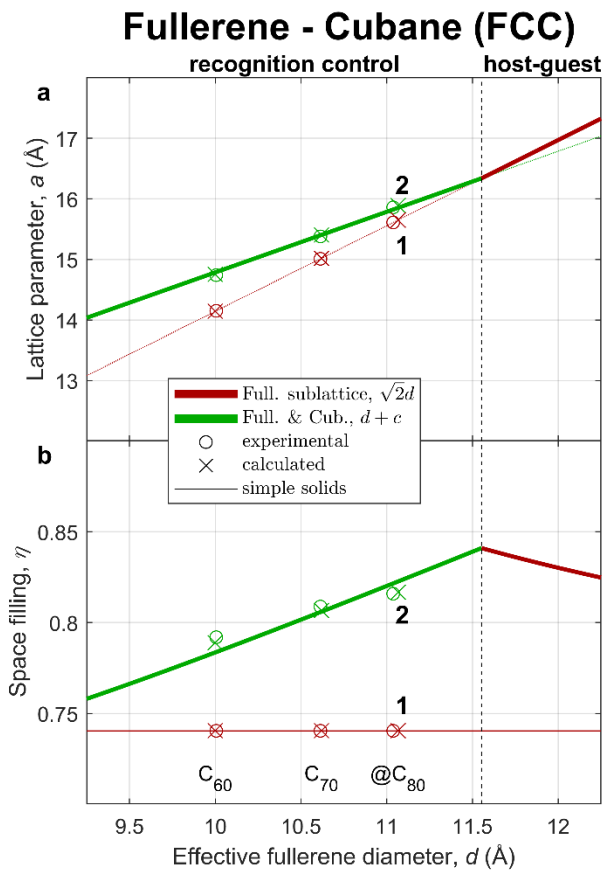

Figure 2. Lattice parameter (a) and space filling (b) of the FCC fullerene-cubane cocrystals as a function of the effective diameter of the fullerenes. The lines correspond to the geometrical model (the 3rd line is out of range), while points are the experimental and calculated values as explained in the discussion. Bold numbers refer to numbering of compounds. All cocrystals are in the recognition-controlled regime.

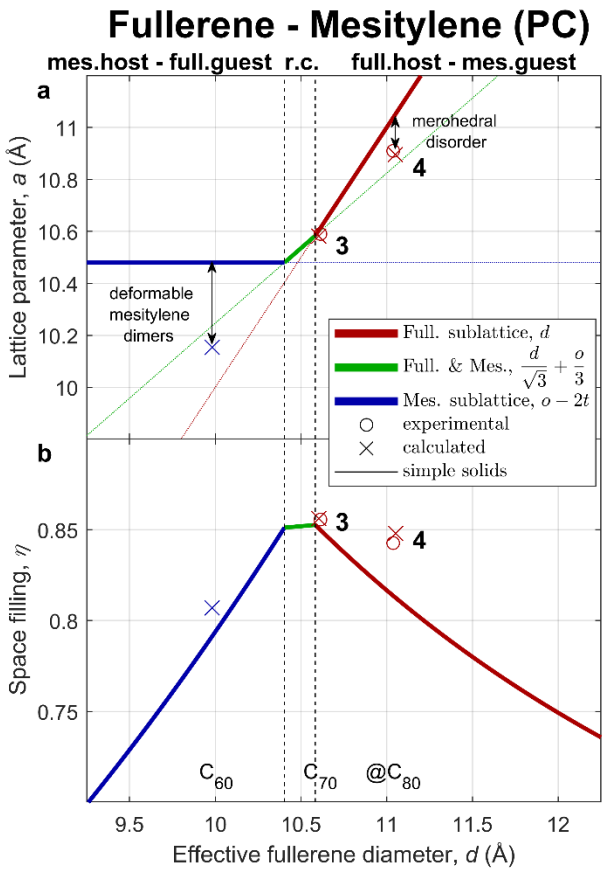

Figure 3. Lattice parameter (a) and space filling (b) of the PC fullerene-mesitylene cocrystals as a function of the effective diameter of the fullerenes. The lines correspond to the geometrical model, while points are the experimental and calculated values as explained in the discussion. Bold numbers refer to numbering of compounds. The existing cocrystals are in the fullerene host – mesitylene dimer guest regime. The geometrical model obviously cannot account for merohedral disorder of fullerenes and non-rigid nature of the mesitylene dimers, explaining the large deviation of the points from the solid line.

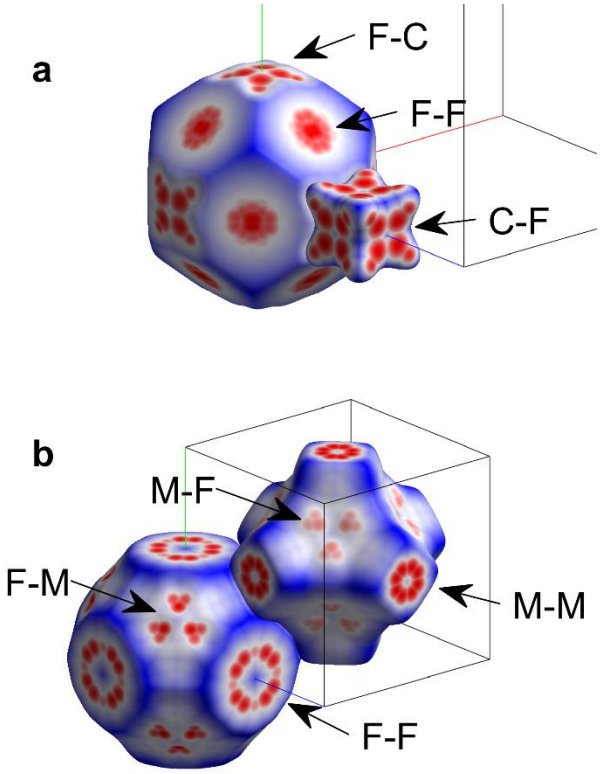

Figure 4. d_{norm} values plotted on Hirshfeld surfaces of (a) FCC $Sc_3N@C_{80}•C_8H_8$ (**2**) and (b) PC $Sc_3N@C_{80}•(C_9H_{12})_2$ (**4**). The boxes indicate the unit cell. F-F, F-C, C-F and F-F, F-M, M-F, M-M annotations refer to interaction regions of the fullerene, cubane and the dimers of mesitylene. Local repulsion and attraction are equally visible in all supramolecular interaction regions; their resultant can be derived from the sublattice optimization within our approach.